Dynamical corrections to transition state theory for multistate systems: Surface self-diffusion in the rare-event regime

Arthur F. Voter and Jimmie D. Doll
Chemistry Division, Los Alamos National Laboratory, Los Alamos, New Mexico 87545

(Received 10 August 1984; accepted 17 September 1984)

We derive an expression for the classical rate constant between any two states of a multistate system. The rate is given as the transition state theory rate of escape from the originating state, multiplied by a dynamical correction factor in the form of a time-correlation function which is evaluated using molecular dynamics techniques. This method is desiged to treat cases in which reactive state-change events are so infrequent (e.g., at low temperature) that direct molecular dynamics calculations are unfeasible. In this regime where dynamical recrossings occur much more quickly than the average time between reactive state changes, the concept of a rate between two nonadjacent states becomes meaningful. We apply the method to the surface diffusion of Rh on Rh(100) at the temperatures employed in field ion microscope experiments.

I. INTRODUCTION

The direct simulation of chemical processes via classical molecular dynamics (MD) techniques is now a widely used and powerful approach,[1] due largely to the high speed of modern computers. There remains, however, a class of systems for which direct molecular dynamics simulation is unfeasible. These systems are characterized by the "rare-event" nature of their dynamical evolution from reactant to product states. Because there is a "bottleneck" in phase space (e.g., a high activation barrier) through which the system must pass to change states, direct integration of the equations of motion may require many years of computer time before a single reactive state-change event is observed. Examples of these rare-event processes include thermal desorption from solid surfaces, surface diffusion at low temperatures, and any chemical reaction with an activation barrier which is high relative to the temperature.

For such systems an elegant alternative approach has been developed,[2-9] which yields exact dynamical quantities without the computational effort growing proportional to the rareness of the event of interest (as in direct MD). The key to this approach is the factoring of the rate constant into two parts: (1) an equilibrium factor, defined as the flux through a dividing surface separating the two states, and (2) a dynamical correction factor, which accounts for the fact that this flux contains spurious crossings which do not correspond to true reactive state-change events. The rare-event nature of the process is included in the first factor, which is simply the transition state theory (TST) rate constant. Because this is an equilibrium property of the system, and does not require knowledge of the dynamics, a variety of methods are available for computing it efficiently.[10,11] The second factor requires explicit use of molecular dynamics, but is easily evaluated because the trajectories need only be followed for relatively short times.

For many problems the dynamical correction factor is close to unity (especially if the TST dividing surface is chosen well), and thus the TST approximation is often very good. Indeed, TST has proven to be, and remains, a most valuable tool for computing reaction rates.[12] However, it is important to have the capability of computing dynamically exact rates for two reasons: (1) the quality of TST can be tested for a certain type of system by comparing to the exact result for a representative case, and (2) for many systems, the TST approximation is too poor to be useful.

Though the concept of a dynamical correction factor has been around for many years,[13] the first use of MD for its exact evaluation was due to Keck.[2] More recently, this type of approach has been applied to describe diffusion in solids,[6] gas phase reactions,[3,4,14,15] intramolecular rearrangements[8,16] and reactions in solution,[9] and thermal desorption from solids.[17-19] All work to date (with two exceptions[16,19] discussed below) has been on two-state systems. In this paper we present a generalization of the dynamical-correction formalism to the many-state case. This should be useful for a variety of problems, such as diffusion on or in a solid, polymer chain dynamics, etc. As an example, we apply the method to calculate the surface self-diffusion rate for a Rh atom on a Rh(100) surface at 300 K, a task which would require $>10^8$ years of computer time[20] using direct MD.

Our derivation of the many-state result is identical in spirit to the two-state formalism presented by Chandler,[8] and Skinner and Wolynes.[9] From the properties of the fluctuation–fluctuation autocorrelation function for a system at equilibrium, they extracted an expression which gives a precise prescription for evaluating the dynamical correction factor using classical trajectories. Montgomery, Holmgren, and Chandler[16] have examined the appropriate time correlation functions to estimate the importance of multiple-state transitions in alkane chains, and

 0021-9606/85/010080-13$02.10

Adams and Doll[19] have derived a matrix formulation for the many-state case, but in neither work did the authors actually extract elementary rate constants. We show here that the elementary rate constants can be extracted and, as in the two-state case, the formalism yields a simple prescription for computing the necessary dynamical correction factors. Moreover, an interesting concept which emerges naturally from this formalism is that of a rate constant between two states which are not adjacent in configuration space.

This paper is organized as follows: We review the two-state derivation in Sec. II, and extend it to the many-state case in Sec. III. Section IV contains a description of how molecular dynamics techniques are applied to compute the dynamical correction factors, and Sec. V contains the application to Rh on Rh(100) surface diffusion.

II. THEORY: TWO-STATE SYSTEM

We first derive the method for making dynamical corrections to transition state theory (TST) for a two-state classical system. This is a simplified version of Chandler's original derivation.[8] As shown in Fig. 1, we are considering a one-dimensional system with two stable configurations, A and B, separated by an energy barrier at $x = q$. We assume that for a canonical ensemble of such systems, a first-order rate law applies, so that

$$\dot{N}_A = -k_{A\to B}N_A + k_{B\to A}N_B$$
$$\dot{N}_B = k_{A\to B}N_A - k_{B\to A}N_B, \tag{2.1}$$

where N_A and N_B are the populations of state A and state B, respectively, $k_{A\to B}$ and $k_{B\to A}$ are the elementary rate constants, and the dot indicates a time derivative. We can define fluctuations of N_A and N_B away from their equilibrium values by

$$\delta N_A = N_A - \bar{N}_A$$
$$\delta N_B = N_B - \bar{N}_B, \tag{2.2}$$

where conservation of particles requires

$$\delta N_A + \delta N_B = 0. \tag{2.3}$$

Combining Eqs. (2.1), (2.2), and (2.3) leads to a rate law for the fluctuations,

$$\begin{aligned}\delta\dot{N}_A(t) &= k_{B\to A}\delta N_B - k_{A\to B}\delta N_A \\ &= -k_{B\to A}\delta N_A - k_{A\to B}\delta N_A \\ &= -k_{\text{eff}}\delta N_A(t),\end{aligned} \tag{2.4}$$

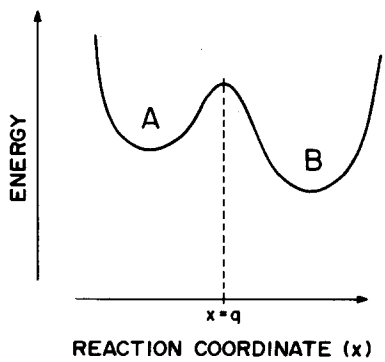

FIG. 1. Energy diagram for one-dimensional two-state system. The boundary between the two states is at $x = q$.

where we have defined an effective rate constant as

$$k_{\text{eff}} = k_{A\to B} + k_{B\to A}. \tag{2.5}$$

Equation (2.4) gives the response of the system to an artificial displacement from equilibrium. From the fluctuation-dissipation theorem,[21] we expect that when the system is at equilibrium, it responds in this same way to spontaneously occurring fluctuations. Thus, we deduce the behavior of the fluctuation–fluctuation autocorrelation function to be

$$\langle\delta N_A(0)\delta\dot{N}_A(t)\rangle = -k_{\text{eff}}\langle\delta N_A(0)\delta N_A(t)\rangle. \tag{2.6}$$

The angular brackets indicate the usual canonical-ensemble average

$$\langle Y\rangle = \frac{\int dp \int dx\, Ye^{-\beta H}}{\int dp \int dx\, e^{-\beta H}},$$

where p is the conjugate momentum, H is the Hamiltonian for the system, and $\beta = 1/k_BT$ (k_B = the Boltzmann constant, T = temperature). Noting that

$$\langle\delta N_A(0)\delta\dot{N}_A(t)\rangle = -\langle\delta\dot{N}_A(0)\delta N_A(t)\rangle,$$

we may rewrite Eq. (2.6) as

$$k_{\text{eff}} = \frac{\langle\delta\dot{N}_A(0)\delta N_A(t)\rangle}{\langle\delta N_A(0)\delta N_A(t)\rangle}. \tag{2.7}$$

Equation (2.7) gives an expression for the dynamically correct rate constant in terms of equilibrium properties, though it is not yet in a particularly useful form.

Noting that the denominator in Eq. (2.7) is a slowly varying function of time compared to the numerator, we make the following approximation, which we discuss later:

$$\langle\delta N_A(0)\delta N_A(t)\rangle \approx \langle\delta N_A(0)\delta N_A(0)\rangle. \tag{2.8}$$

With this assumption, and making use of Eq. (2.3), Eq. (2.7) becomes

$$k_{\text{eff}}(t) = \frac{-\langle\delta\dot{N}_A(0)\delta N_B(t)\rangle}{\langle\delta N_A(0)\delta N_A(0)\rangle}, \tag{2.9}$$

where we have explicitly indicated the time dependence of k_{eff}. Without loss of generality, we can make the simplifying requirement that

$$N_A + N_B = 1,$$

so that

$$N_A(t) = \theta[q - x(t)],$$
$$N_B(t) = \theta[x(t) - q],$$

where θ is the standard step function. The fluctuations in N_A and N_B are thus given by

$$\delta N_A(t) = \theta[q - x(t)] - \chi_A$$
$$\delta N_B(t) = \theta[x(t) - q] - \chi_B, \tag{2.10}$$

where χ_A and χ_B are the equilibrium mole fractions of components A and B, respectively (note that $\chi_A = \bar{N}_A$,

$\chi_B = \bar{N}_B$). The autocorrelation function in the denominator of Eq. (2.9) becomes

$$\begin{aligned}\langle \delta N_A(0)\delta N_A(0)\rangle &= \langle\{\theta[q - x(0)] - \chi_A\}\{\theta[q - x(0)] - \chi_A\}\rangle \\ &= \langle\theta[q - x(0)]\theta[q - x(0)]\rangle - \chi_A^2 \\ &= \chi_A - \chi_A^2. \end{aligned} \tag{2.11}$$

From detailed balance, we know that

$$\frac{k_{A\to B}}{k_{B\to A}} = \frac{\chi_B}{\chi_A}$$

so that Eq. (2.5) becomes

$$k_{\text{eff}} = k_{A\to B}\left(1 + \frac{\chi_A}{\chi_B}\right),$$

and from Eqs. (2.9) and (2.11) we have

$$\begin{aligned} k_{A\to B}(t) &= \frac{-\langle \delta\dot{N}_A(0)\delta N_B(t)\rangle}{[1 + (\chi_A/\chi_B)](\chi_A - \chi_A^2)} \\ &= \frac{-\langle \delta\dot{N}_A(0)\delta N_B(t)\rangle}{\chi_A}. \end{aligned} \tag{2.12}$$

To simplify the numerator of Eq. (2.12), we need the time derivative of δN_A; from Eq. (2.10) we have

$$\delta\dot{N}_A(0) = -\dot{x}(0)\delta[q - x(0)],$$

where $\delta(\cdots)$ indicates the Dirac delta function. Thus, we obtain

$$k_{A\to B}(t) = \frac{\langle \dot{x}(0)\delta[x(0) - q]\theta[x(t) - q]\rangle}{\chi_A}. \tag{2.13}$$

The numerator in Eq. (2.13) can be interpreted as the particle flux through the $x = q$ dividing surface, modified by the step function $\theta[x(t) - q]$. The particles crossing the dividing surface in the $+x$ direction (i.e., moving from state A to state B) at time zero that reside in state B at time t contribute positively to the ensemble average, while particles residing in state B at time t that were making a $-x$ crossing at time zero contribute negatively to the average.

If every particle that crosses the dividing surface in the $+x$ direction remains in state B (at least until a time greater than t), and every particle crossing in the $-x$ direction remains in state A, then the ensemble average in Eq. (2.13) is simply the one-directional flux through the dividing surface. This is the transition state theory (TST) assumption, that every dividing surface crossing corresponds to a reactive state change. We can modify Eq. (2.13) to reflect the TST approximation by setting t to some small value ϵ, chosen such that no recrossings can occur between $t = 0$ and $t = \epsilon$. This gives

$$\begin{aligned} k_{A\to B}^{\text{TST}} &= \frac{\langle \dot{x}(0)\delta[x(0) - q]\theta[x(\epsilon) - q]\rangle}{\chi_A} \\ &= \frac{\langle \dot{x}(0)\delta[x(0) - q]\theta[\dot{x}(0)]\rangle}{\chi_A}. \end{aligned} \tag{2.14}$$

It is easy to show that Eq. (2.14) is equivalent to a more familiar expression for the TST rate. Noting first that, in a canonical ensemble, the forward and reverse flux through $x = q$ have equal magnitudes, we can write

$$k_{A\to B}^{\text{TST}} = \frac{\frac{1}{2}\langle|\dot{x}(0)|\delta[x(0) - q]\rangle}{\chi_A}. \tag{2.15}$$

We can express χ_A as

$$\begin{aligned}\chi_A &= \langle\theta[q - x(0)]\rangle \\ &= \frac{\int dp \int dx\, \theta[q - x(0)]e^{-\beta H(x,p)}}{\int dp \int dx\, e^{-\beta H(x,p)}} \\ &= \frac{\int dp \int_A dx\, e^{-\beta H(x,p)}}{\int dp \int_{A+B} dx\, e^{-\beta H(x,p)}}, \end{aligned}$$

where the subscripts A and A + B indicate that the configuration-space integrals are over state A and all space, respectively. Equation (2.15) thus becomes

$$\begin{aligned} k_{A\to B}^{\text{TST}} &= \left[\left[\frac{1}{2}\frac{\int dp \int_{A+B} dx|\dot{x}(0)|\delta[x(0) - q]e^{-\beta H}}{\int dp \int_{A\to B} dx\, e^{-\beta H}}\right]\right. \\ &\quad \left.\times\left[\frac{\int dp \int_{A+B} dx\, e^{-\beta H}}{\int dp \int_A dx\, e^{-\beta H}}\right]\right] \\ &= \frac{1}{2}\langle|\dot{x}(0)|\delta[x(0) - q]\rangle_A, \end{aligned} \tag{2.16}$$

where the subscript A indicates that the configuration space part of the ensemble average is integrated only over state A (plus the infinitesimal region necessary to include the TST dividing surface). Equation (2.16) is a standard expression for $k_{A\to B}^{\text{TST}}$,[8,11,22] interpretable as the flux of particles through the TST dividing surface bordering state A, divided by two since half the flux is going the wrong direction. Note that the expression is independent of the nature of state B[23]; $k_{A\to B}^{\text{TST}}$ is simply the *rate of escape* from state A across the boundary surface.

The dynamical correction factor we seek is obtained by taking the ratio of $k_{A\to B}$ [Eq. (2.13)] to $k_{A\to B}^{\text{TST}}$ [Eq. (2.14)], which yields

$$f_d(t) = \frac{k_{A\to B}}{k_{A\to B}^{\text{TST}}} = \frac{\langle \dot{x}(0)\delta[x(0) - q]\theta[x(t) - q]\rangle}{\langle \dot{x}(0)\delta[x(0) - q]\theta[x(\epsilon) - q]\rangle}. \tag{2.17}$$

Implementation of Eq. (2.17) requires an understanding of the time dependence of the correlation function in the numerator. As mentioned above, the TST assumption that every particle crossing the dividing surface will come to rest without recrossing is invalid for many systems. After a crossing, there is a chance that the particle will recross the surface one or more times before ultimately

thermalizing in state A or state B. (We are assuming that the system is coupled to other degrees of freedom, which are constantly exchanging energy with the coordinate considered explicitly.) We define τ_{corr} as the time scale on which these correlated dynamical recrossing events occur; i.e., a particle crossing $x = q$ at time zero will have thermalized by time τ_{corr}. We also define a time scale associated with the reaction, $\tau_{rxn} \approx (k_{eff})^{-1}$, which corresponds to the average time between *reactive* crossings of the dividing surface. At very short times ($t \leqq \epsilon$), the dynamical correction factor given by Eq. (2.17) is unity, since the numerator and denominator are equivalent. As t is increased to τ_{corr}, $f_d(t)$ decays to some value less than one, because trajectories which recross contribute negatively, or fail to contribute, to the numerator. If τ_{rxn} is much greater than τ_{corr}, then $f_d(t)$ will reach a plateau value at $t = \tau_{corr}$, as shown in Fig. 2. If $f_d(t)$ is examined on a very long time scale (i.e., units of τ_{rxn}), it will be seen to decay exponentially, and it ultimately tends to zero, because the direction of travel of a particle making a crossing at time zero is uncorrelated with its position at $t \gg \tau_{rxn}$. Thus, only if this plateau region exists, and if Eq. (2.17) is evaluated during that time, can meaningful results be obtained. The dynamically correct rate constant will be given by

$$k_{A\to B} = k^{TST}_{A\to B} f_d(t_p), \tag{2.18}$$

where t_p satisfies

$$\tau_{corr} < t_p \ll \tau_{rxn}. \tag{2.19}$$

We can now examine the approximation made in Eq. (2.8). Because the correlation function $\langle \delta N_A(0) \delta N_A(t) \rangle$ decays on a time scale of τ_{rxn}, and because we restrict ourselves to times much smaller than τ_{rxn}, the zero time assumption is perfectly reasonable. Note that Eq. (2.7), which does not include this assumption, gives an expression for the dynamically correct rate constant which is valid for *all* times greater than τ_{corr}. As the numerator in Eq. (2.7) decays towards zero for $t \gg \tau_{rxn}$, the denominator also decays, leading to a constant ratio. Thus, if we used Eq. (2.7) to compute k_{eff}, we would not need to require a separation of time scales between τ_{corr} and τ_{rxn}; we could simply pick any $t > \tau_{corr}$ to evaluate the right-hand side of Eq. (2.7). However, evaluating the denominator of Eq. (2.7) requires more computational work than the numerator, and can become prohibitively expensive when the reaction is slow. For this reason Eq. (2.17) becomes the method of choice when the requirements of Eq. (2.19) can be met.

The concept of time-scale separation merits further discussion. We can view this approach to calculating $k_{A\to B}$ in the following way: We imagine watching the motion of a single particle which has resided in state A for a time greater than τ_{corr}. When that particle finally makes a crossing of the dividing surface, we close our eyes for the next τ_{corr} time units, and then note the state of the particle upon reopening our eyes. If the particle is in state B, we say that a reactive crossing has occurred, but if the particle is in state A, we pretend that nothing happened—the particle never left state A. We now continue to monitor the motion of this particle, and follow the same prescription each time a crossing occurs (in either direction). After observing a large number of reactive hops, we can compute $k_{A\to B}$ as the average of the inverse of the time between a reactive hop into state A and the subsequent reactive exit from state A. Because $\tau_{corr} \ll \tau_{rxn}$, we make only a negligible error using this approach—there is a negligible probability that an important event (i.e., an extra reactive crossing) occurs during the infinitesimal fraction of time that our eyes are closed.

Now consider how Eq. (2.17) actually performs this counting. Figure 3 shows an idealized plot of the time evolution of a system executing the four possible types of surface crossings: A → B, A → A, B → A, and B → B, each consisting of multiple recrossings. Only the A → B event [Fig. 3(a)] should contribute to the calculation of $k_{A\to B}$. If we examine a canonical ensemble of particles at a given instant of time, we find that each of the five crossings in Fig. 3(a) are present. The time-correlation function $\langle \dot{x}(0) \delta[x(0) - q] \theta[x(t_p) - q] \rangle$ instructs us to allow each of these five systems to evolve for a time τ_{corr}, and then examine the final state. Because each system in our example will be in state B, so that $\theta[x(t_p) - q] = 1$, they will contribute positively or negatively to the average, depending on the sign of $\dot{x}(0)$. Crossings 1, 3, and 5 contribute positively, while 2 and 4 contribute negatively. Thus, the net contribution will be one crossing, as will be the case for any number of recrossings. [Note that only the *phase* of $\dot{x}(0)$ is important, not the magnitude;

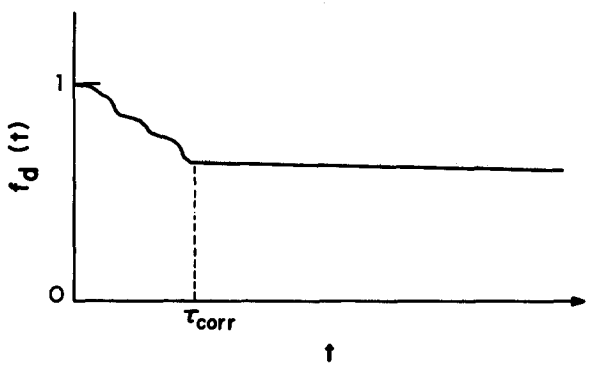

FIG. 2. Typical behavior of the two-state dynamical correction factor [Eq. (2.17)] for $\tau_{corr} \ll \tau_{rxn}$.

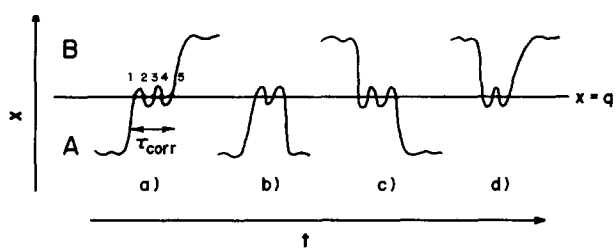

FIG. 3. Idealized diagram of the four possible multiple-crossing events for the two-state system. The numbers 1 to 5 in (a) label the five crossings that comprise the single A → B reactive crossing event. The A → A, B → A, and B → B crossing events shown in (b), (c), and (d) make zero contribution to the numerator in Eq. (2.17), and hence do not contribute to the dynamically correct $k_{A\to B}$.

the magnitude appears in the ensemble average because we are sampling from a velocity-weighted Boltzmann distribution, corresponding to a snapshot in time of the particles crossing the dividing surface. This will be demonstrated in Sec. IV.] The A → A and B → A events shown in Figs. 3(b) and 3(c) contribute nothing to the average because $\theta[x(t) - q] = 0$. The B → B event shown in Fig. 3(d) makes no net contribution to the average because there are an equal number of $\dot{x}(0) > 0$ and $\dot{x}(0) < 0$ crossings.

Computation of the dynamically exact classical rate constant is accomplished in two stages. First, the TST rate constant is evaluated via Eqs. (2.15) or (2.16). Then the dynamical correction factor f_d is computed from Eq. (2.17), using the same dividing surface as in the TST calculation. The ensemble averages in Eq. (2.17) are evaluated by following the behavior of a swarm of classical trajectories which start from the TST dividing surface. This procedure is described in detail in Sec. IV. It is worth noting that the rate constant computed in this manner is independent of the location of the dividing surface. While choosing the surface to be at the free-energy maximum between the two states will yield the most accurate $k_{A\to B}^{TST}$ (and f_d closest to unity), other positions will also work. This is helpful in many-dimensional systems, because the position which will maximize f_d is often not easily defined.

III. THEORY: MULTISTATE SYSTEM

In the last section we showed that the dynamical correction factor for a two-state system can be expressed as a ratio of equilibrium correlation functions, which may be evaluated using classical trajectory techniques. In this section we extend the analysis to a system with an arbitrary number of states, and with the same assumption that $\tau_{corr} \ll \tau_{rxn}$, we show that an analogous expression exists for the rate of reaction between any two states of the system.

We begin with the matrix formulation of the rate law used by Adams and Doll.[19] The system is assumed to be composed of n states, with no restriction on the connectivity of the states. An example is the potential for an atom diffusing on a solid surface. In this case, there are an infinite number of states, each corresponding to one binding site, with each state bordering between two and four other states (depending on the crystal face). Because the total number of particles N is held fixed, it is sufficient to specify the populations of $n - 1$ states. We thus define the $(n - 1)$-dimensional column vector of time-dependent populations $\mathbf{N}(t)$ and fluctuations away from equilibrium,

$$\delta\mathbf{N}(t) = \mathbf{N}(t) - \bar{\mathbf{N}}, \tag{3.1}$$

where $\bar{\mathbf{N}}$ is the column vector of equilibrium populations. We again assume that the populations, and hence the fluctuations, obey a first-order rate law, which we may write as

$$\delta\dot{\mathbf{N}}(t) = -\mathsf{k}\delta\mathbf{N}(t), \tag{3.2}$$

where k is a $(n - 1) \times (n - 1)$ matrix of rate constants. It is important to note that the elements of k are *not* the elementary rate constants (indeed, our task will be to find the relation between the two). As in the two-state case, we take the behavior of the fluctuation correlation functions to be governed by the same rate law, leading to

$$\langle\delta\dot{\mathbf{N}}(t)\delta\mathbf{N}^T(0)\rangle = -\mathsf{k}\langle\delta\mathbf{N}(t)\delta\mathbf{N}^T(0)\rangle,$$

which was obtained by right multiplying Eq. (3.2) by the row vector $\delta\mathbf{N}^T(0)$ [the transpose of $\delta\mathbf{N}(0)$], and taking an ensemble average. [Note that $\langle\delta\mathbf{N}(t)\delta\mathbf{N}^T(0)\rangle$ represents a matrix of correlation functions.] Taking advantage of

$$\langle\delta\dot{\mathbf{N}}(t)\delta\mathbf{N}^T(0)\rangle = [\langle\delta\mathbf{N}(0)\delta\dot{\mathbf{N}}^T(t)\rangle]^T$$

and

$$\langle\delta\mathbf{N}(0)\delta\dot{\mathbf{N}}^T(t)\rangle = -\langle\dot{\mathbf{N}}(0)\delta\mathbf{N}^T(t)\rangle,$$

we obtain an expression for the elements of the transpose of k,

$$\mathsf{k}^T = [\langle\delta\mathbf{N}(0)\delta\mathbf{N}^T(t)\rangle]^{-1}\langle\delta\dot{\mathbf{N}}(0)\delta\mathbf{N}^T(t)\rangle. \tag{3.3}$$

We now deviate from Adams and Doll.

We wish to express the *elementary* rate constants $k_{i\to j}^{el}$ in terms of time correlation functions, as we did for the two-state case. We can write the rate law as

$$\begin{aligned}\delta\dot{N}_i(t) &= \sum_j^n (-\delta N_i k_{i\to j}^{el} + \delta N_j k_{j\to i}^{el}) \\ &= -\sum_j^n \delta N_i f_{ij} + \sum_j^n \delta N_j f_{ji},\end{aligned} \tag{3.4}$$

where δN_i is the ith element of $\delta\mathbf{N}(t)$, and we have introduced the $n \times n$ matrix of elementary rate constants f defined by

$$(\mathsf{f})_{ij} = f_{ij} = k_{i\to j}^{el}, \tag{3.5}$$

to avoid confusing $k_{i\to j}^{el}$ with an element of k. Now consider the following expression, which gives k in terms of elementary rates:

$$(\mathsf{k})_{ij} = -f_{ji} + f_{ni} + \delta_{ij}\sum_k^n f_{ik}; \quad i, j < n \tag{3.6}$$

(here δ_{ij} is the Kronecker delta function). We will prove Eq. (3.6) by inserting it into Eq. (3.2) and comparing with Eq. (3.4). Rewriting Eq. (3.2) and inserting Eq. (3.6) gives

$$\begin{aligned}\delta\dot{N}_i(t) &= -\sum_k^{n-1} (\mathsf{k})_{ik}\delta N_k(t) \\ &= -\sum_k^{n-1}\left(-f_{ki} + f_{ni} + \delta_{ik}\sum_l^n f_{il}\right)\delta N_k(t) \\ &= \sum_k^{n-1} f_{ki}\delta N_k(t) - f_{ni}\sum_k^{n-1}\delta N_k(t) - \sum_k^n f_{ik}\delta N_i(t).\end{aligned}$$

Extending the range of the first two sums from $n - 1$ to n (the extra terms cancel), and noting that

$$\sum_k^n \delta N_k(t) = 0 \tag{3.7}$$

we obtain

$$\delta\dot{N}_i(t) = \sum_k^n f_{ki}\delta N_k(t) - 0 - \sum_k^n f_{ik}\delta N_i(t),$$

which is the same as Eq. (3.4), proving Eq. (3.6). Now consider another expression:

$$k_{i\to j}^{\mathrm{el}} = f_{ij} = \sum_k^{n-1} \chi_k(\mathsf{k})_{jk} - (\mathsf{k})_{ji}; \quad i,j < n, \tag{3.8}$$

where χ_k is the equilibrium mole fraction in state k. We will prove this by inserting Eq. (3.6) into the right-hand side of Eq. (3.8), which gives

$$\sum_k^{n-1} \chi_k\left(-f_{kj} + f_{nj} + \delta_{jk}\sum_l^n f_{jl}\right) + f_{ij} - f_{nj} - \delta_{ji}\sum_k^n f_{jk}.$$

Because we are not interested in $k_{i\to i}^{\mathrm{el}}$, we may discard the last term ($\delta_{ji}\sum_k^n f_{jk}$). We may also extend the range of the first sum from $n-1$ to n, because the extra terms cancel, as long as $j < n$. (We are currently restricting i and j to be less than n, but our ultimate expression for $k_{i\to j}^{\mathrm{el}}$ will be valid for all $i \neq j$.) This leads to

$$-\sum_k^n \chi_k f_{kj} + f_{nj}\sum_k^n \chi_k + \sum_l^n f_{jl}\chi_j + f_{ij} - f_{nj},$$

and using

$$\sum_k^n \chi_k = 1$$

and

$$\chi_i f_{ij} = \chi_j f_{ji},$$

we obtain

$$\sum_k^n(-\chi_k f_{kj} + \chi_j f_{jk}) + f_{nj}\left(\sum_k^n \chi_k\right) + f_{ij} - f_{nj}$$
$$= 0 + f_{nj} + f_{ij} - f_{nj}$$
$$= f_{ij},$$

which proves Eq. (3.8). Substituting Eq. (3.3) into Eq. (3.8) gives the elementary rate constants in terms of correlation functions, but first we wish to simplify the "denominator" matrix in Eq. (3.3).

As in the two-state case, we will approximate the fluctuation–fluctuation correlation function by its time-zero value

$$\langle\delta\mathbf{N}(0)\delta\mathbf{N}^T(t)\rangle \approx \langle\delta\mathbf{N}(0)\delta\mathbf{N}^T(0)\rangle. \tag{3.9}$$

Taking $N = 1$ (with no loss of generality), so that $\bar{N}_i = \chi_i$, it is easy to show (see the Appendix) that

$$[\langle\delta\mathbf{N}(0)\delta\mathbf{N}^T(0)\rangle]_{ij} = \delta_{ij}\chi_i = \chi_i\chi_j, \tag{3.10}$$

and that the desired inverse matrix is given by

$$\{[\langle\delta\mathbf{N}(0)\delta\mathbf{N}^T(0)\rangle]^{-1}\}_{ij} = \frac{1}{\chi_n} + \frac{\delta_{ij}}{\chi_i}. \tag{3.11}$$

Using Eqs. (3.3), (3.8), and (3.11), we can express the elementary rate constants in terms of the correlation-function matrix elements

$$C_{ij} = \langle\delta\dot{N}_i(0)\delta N_j(t)\rangle.$$

From Eqs. (3.3) and (3.11) we have

$$(\mathbf{k}^T)_{ij} = \sum_k^{n-1}\left(\frac{1}{\chi_n} + \frac{\delta_{ik}}{\chi_i}\right)C_{kj},$$

so that

$$(\mathbf{k})_{ij} = \sum_k^{n-1}\left(\frac{1}{\chi_n} + \frac{\delta_{jk}}{\chi_j}\right)C_{ki},$$

and inserting into Eq. (3.8) gives

$$k_{i\to j}^{\mathrm{el}} = \sum_l^{n-1}\chi_l\left[\sum_k^{n-1}\left(\frac{1}{\chi_n} + \frac{\delta_{lk}}{\chi_l}\right)C_{kj}\right] - \sum_k^{n-1}\left(\frac{1}{\chi_n} + \frac{\delta_{ik}}{\chi_i}\right)C_{kj}$$
$$= \left(\sum_l^{n-1}\chi_l\right)\left(\sum_k^{n-1}\frac{C_{kj}}{\chi_n}\right) + \sum_l^{n-1}\frac{\chi_l}{\chi_l}C_{lj} - \sum_k^{n-1}\frac{C_{kj}}{\chi_n} - \frac{C_{ij}}{\chi_i}$$
$$= \left(\frac{1-\chi_n}{\chi_n}\right)\sum_k^{n-1}C_{kj} + \sum_k^{n-1}C_{kj} - \frac{1}{\chi_n}\sum_k^{n-1}C_{kj} - \frac{C_{ij}}{\chi_i}$$
$$= -C_{ij}/\chi_i,$$

and substituting for C_{ij} yields

$$k_{i\to j}^{\mathrm{el}} = \frac{-\langle\delta\dot{N}_i(0)\delta N_j(t)\rangle}{\chi_i}. \tag{3.12}$$

Equation (3.12) is the central result of this paper. It states that, when $\tau_{\mathrm{corr}} \ll \tau_{\mathrm{rxn}}$, the elementary rate constant between any two states, connected or not, is given by a simple equilibrium correlation function. Note that the form of Eq. (3.12) is identical to Eq. (2.12) for the two-state system. Note also that there is no dependence on state n in Eq. (3.12); we are free to choose any state other than i or j as the nth state, and thus we may abandon the $i, j < n$ restriction. As in the two-state case, we will tinker with Eq. (3.12) to obtain a computationally convenient form.

Because systems of interest will rarely be one dimensional, we extend our scope to a many-dimensional system defined by the coordinate $\mathbf{R}$. The time-dependent population of state i is given by

$$\theta_i(t) = \theta\{F_i[\mathbf{R}(t)]\},$$

where $F_i(\mathbf{R})$ is a continuous, differentiable function with the property that

$$F_i(\mathbf{R}) \begin{cases} >0, & \text{if } \mathbf{R} \text{ is in state } i, \\ =0, & \text{if } \mathbf{R} \text{ is on the boundary to state } i, \\ <0, & \text{if } \mathbf{R} \text{ is outside state } i. \end{cases}$$

The population fluctuation is thus

$$\delta N_i(t) = \theta_i(t) - \chi_i \tag{3.13}$$

and the time derivative becomes

$$\delta\dot{N}_i(t) = \delta\{F_i[\mathbf{R}(t)]\}\nabla F_i \cdot \mathbf{v}$$
$$= -\delta_i(t)v_i(t), \tag{3.14}$$

where v_i is the velocity normal to the dividing surface (defined as positive when the system is *exiting* state i),

$$v_i = \frac{-\nabla F_i \cdot \mathbf{v}}{|\nabla F_i|},$$

and we have defined

$$\delta_i(t) = \delta\{F_i[\mathbf{R}(t)]\}|\nabla F_i[\mathbf{R}(t)]|. \tag{3.15}$$

Equation (3.12) becomes

$$k_{i\to j}^{\mathrm{el}} = \frac{\langle v_i(0)\delta_i(0)\theta_j(t)\rangle}{\chi_i}, \tag{3.16}$$

and writing the TST rate of *escape* from state i as

$$k_{i\to}^{\mathrm{TST}} = \frac{\frac{1}{2}\langle|v_i(0)|\delta_i(0)\rangle}{\chi_i} \tag{3.17}$$

[see Eq. (2.15)], we obtain

$$k_{i\to j}^{\mathrm{el}} = \frac{\langle v_i(0)\delta_i(0)\theta_j(t)\rangle}{\frac{1}{2}\langle|v_i(0)|\delta_i(0)\rangle} k_{i\to}^{\mathrm{TST}}. \tag{3.18}$$

As in the two-state case, we have expressed the true rate constant as the transition state theory rate modified by a ratio of ensemble averages. The expression is only valid if the numerator can be evaluated at a time t such that

$$\tau_{\mathrm{corr}} < t \ll \tau_{\mathrm{rxn}}. \tag{3.19}$$

Before describing how to evaluate Eq. (3.18) via molecular dynamics, we conclude this section with a few important points.

As indicated by Eq. (3.17), $k_{i\to}^{\mathrm{TST}}$ depends only on the nature of state i, and the shape of its boundary surface. Thus, in computing $k_{i\to j}^{\mathrm{el}}$, the same TST rate constant is employed for any final state j. All dependence on state j is contained in the time-correlation function $\langle v_i(0)\delta_i(0)\theta_j(t)\rangle$, which accounts for the ultimate fate of particles which are at the boundary to state i at time zero.

Note that state i and state j *need not be connected;* $k_{i\to j}^{\mathrm{el}}$ may be computed from Eq. (3.18) for any two states of the system. While this may seem contrary to the conventional concept of a rate constant, we feel that $k_{i\to j}^{\mathrm{el}}$ is in fact well defined for nonadjacent i and j. As in the two-state case, we appeal to the notion of "closing our eyes" during the time τ_{corr} following an initial crossing event. If a particle initially in state i exits and reappears in some distant state j when we reopen our eyes, then it is reasonable to say that it has made a direct flight from state i to state j. The possibility that we are missing some important event is negligibly small, since our eyes are closed only $\tau_{\mathrm{corr}}/\tau_{\mathrm{rxn}}$ of the time. This concept can also be stated another way. Though states i and j are not connected in configuration space, we can think of them as being connected by a sort of "tunnel" in phase space, which passes through the states connecting i and j. When a particle exits state i with the right set of phase-space coordinates for entering this tunnel, it is automatically guided to state j. Even though it passes through the configuration space of some state k, this tunnel region of phase space is inaccessible to state k, and can only be entered from state i (or state j, by time-reversal symmetry—assuming that all coordinates are explicitly included in the system). A particle can pass from i to j through this tunnel in a time less than τ_{corr}, while actually hopping from i to k, and then k to j, would require $\sim 2\,\tau_{\mathrm{rxn}}$.

As in the two-state case, it is easy to visualize how the ensemble average in Eq. (3.18) counts only the true reactive events. Figure 4 shows a schematic trajectory which, in time τ_{corr}, passes from state i through states k, l, and m, and into state j. Each of the crossing points, labeled 1 to 7, will appear in the canonical ensemble, and after evolving for time τ_{corr}, will reside in state j. Because of the form of the time-correlation function $\langle v_i(0)\delta_i(0)\theta_j(t)\rangle$, this set of trajectories can only contribute to $k_{i\to j}^{\mathrm{el}}$, $k_{k\to j}^{\mathrm{el}}$, $k_{l\to j}^{\mathrm{el}}$, and $k_{m\to j}^{\mathrm{el}}$. However, the net contributions to $k_{k\to j}^{\mathrm{el}}$, $k_{l\to j}^{\mathrm{el}}$, and $k_{m\to j}^{\mathrm{el}}$ will be zero because for each of these three initial states, there are an equal number of initially entering trajectories [$v_i(0) < 0$] and initially exiting trajectories [$v_i(0) > 0$]. (For example, trajectories 4 and 6 contribute negatively to $k_{m\to j}^{\mathrm{el}}$, while 5 and 7 contribute positively.) Thus, as we would hope, the only nonzero contribution is to $k_{i\to j}^{\mathrm{el}}$.

Figure 5 shows the expected time dependence of the dynamical correction factor, defined as

$$f_d(i \to j) = k_{i\to j}^{\mathrm{el}}/k_{i\to}^{\mathrm{TST}}. \tag{3.20}$$

If states i and j are adjacent, the behavior is similar to the two-state case; $f_d(i \to j)$ decays from unity and reaches a plateau value by $t = \tau_{\mathrm{corr}}$. If states i and j are not adjacent, $f_d(i \to j)$ is initially zero (because a finite amount of time is required for any trajectory initially exiting state i to reach state j), and then *rises* towards a plateau value at τ_{corr}. For both cases, the approach to the plateau value is not necessarily a monotonic function, since trajectories passing through state j on their way to another final state will cause a temporary increase (or decrease) in $f_d(i \to j)$

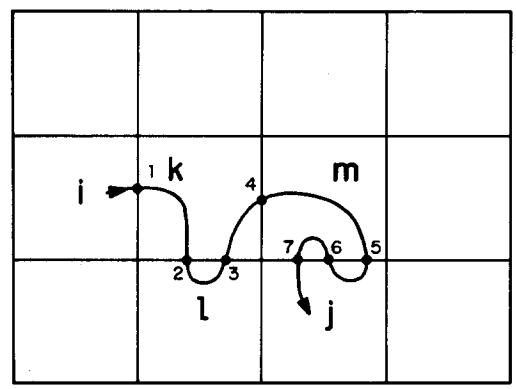

FIG. 4. Schematic example of a trajectory that passes from state i to state j in time τ_{corr}, via states k, l, and m. Each box represents a different state of the system. Each of the seven surface crossings shown will be represented in the canonical ensemble. Using Eq. (3.18) to evaluate the dynamically correct rate constants shows that this trajectory contributes only to $k_{i\to j}$, while at the TST level of approximation this trajectory contributes to $k_{i\to k}^{\mathrm{TST}}$, $k_{k\to i}^{\mathrm{TST}}$, $k_{k\to l}^{\mathrm{TST}}$, $k_{l\to k}^{\mathrm{TST}}$, $k_{k\to m}^{\mathrm{TST}}$, $k_{m\to k}^{\mathrm{TST}}$, $k_{m\to j}^{\mathrm{TST}}$, and $k_{j\to m}^{\mathrm{TST}}$.

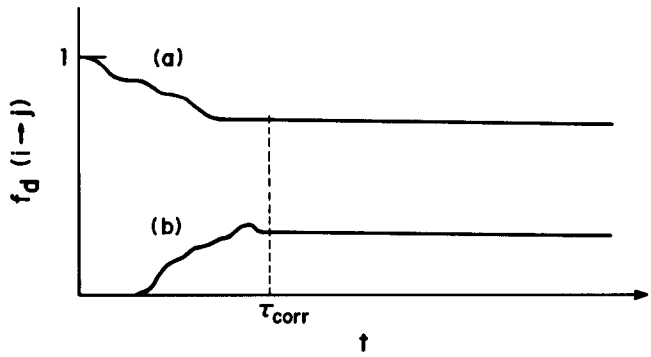

FIG. 5. Typical behavior of the many-state dynamical correction factor [Eq. (3.20)] for $\tau_{corr} \ll \tau_{rxn}$. In case (a), state j is adjacent to state i, and the behavior is very similar to the two-state case. In case (b), states i and j are not adjacent, so that the correction factor is initially zero, and rises to a plateau value.

(this is also true for the two-state case). As in the two-state case, if the time-zero approximation [Eq. (3.9)] had not been imposed, the computed value for $f_d(i \to j)$ would remain constant for all $t > \tau_{corr}$, and the requirement that $\tau_{corr} \ll \tau_{rxn}$ would not be necessary (though this approach would require as much work as a direct molecular dynamics calculation). While in the two-state case this time-zero approximation caused a slow exponential decay in the plateau region, in the many-state case the plateau behavior is more complicated (though still slow), since a number of terms arising from the matrix multiplication shown in Eq. (3.3) are missing.

IV. EVALUATION OF THE RATE CONSTANTS VIA MOLECULAR DYNAMICS

The first stage in calculating $k_{i\to j}^{el}$ consists of computing the TST rate $k_{i\to}^{TST}$. This can be accomplished via Eq. (3.17), or from an ensemble average over only the phase space belonging to state i,

$$k_{i\to}^{TST} = \frac{1}{2}\langle |v_i(0)|\delta_i(0)\rangle_i. \tag{4.1}$$

We have shown elsewhere[24] that this can usually be further simplified to give an average over only the *configuration space* of state i,

$$k_{i\to}^{TST} = \frac{1}{2}\left(\frac{2k_BT}{\pi m}\right)^{1/2}\langle \delta_i(0)\rangle_i, \tag{4.2}$$

where $\delta_i(0)$ is given by Eq. (3.15), and m is the particle mass, assuming that $F_i(\mathbf{R})$ (i.e., the dividing surface) involves the coordinates of one particle only. If $F_i(\mathbf{R})$ is a function of the coordinates of more than one particle, the separation implied by Eq. (4.2) is still possible provided that the effective mass[25] of the coordinate perpendicular to the dividing surface is constant over the whole dividing surface. For this case, the mass in Eq. (4.2) is replaced by the effective mass of this perpendicular coordinate $[S(\mathbf{R})]$, and the gradient operator in Eq. (3.15) operates with respect to S rather than $\mathbf{R}$, so that

$$\delta_i(t) = \delta(F_i)\left|\frac{\partial F_i}{\partial S}\right|. \tag{4.3}$$

Equation (4.2) may be evaluated using Metropolis Monte Carlo techniques,[26–28] once a form for the potential energy function has been chosen. The Monte Carlo approach has the advantage that the exact TST rate is obtained, with statistical error bars that can be made arbitrarily small. Alternatively, some form of harmonic approximation may be employed; this tends to work very well at low temperature where the system resides predominately in the harmonic region of the potential.

The second stage, which is the focus of this section, is the evaluation of the dynamical correction factors. (Either f_d or k^{TST} may be evaluated first; the only requirement is that the *same* TST dividing surface be used for each calculation.) If we define the weighting function for a Maxwellian-flux distribution at the boundary to state i by

$$w_i(\mathbf{R}, \mathbf{p}) = |v_i(0)|\delta_i(0)e^{-\beta H(\mathbf{R},\mathbf{p})} \tag{4.4}$$

(i.e., w_i corresponds to a snapshot of the particles crossing the dividing surface), Eq. (3.18) becomes

$$k_{i\to j}^{el} = \frac{2\int\int \frac{v_i(0)}{|v_i(0)|}\theta_j(t)w_i\,d\mathbf{R}\,d\mathbf{p}\Big/\int\int e^{-\beta H}\,d\mathbf{R}\,d\mathbf{p}}{\int\int w_i\,d\mathbf{R}\,d\mathbf{p}\Big/\int\int e^{-\beta H}\,d\mathbf{R}\,d\mathbf{p}}k_{i\to}^{TST}$$
$$= 2\left\langle\frac{v_i(0)}{|v(0)|}\theta_j(t)\right\rangle_{w_i}k_{i\to}^{TST}, \tag{4.5}$$

where the subscript w_i indicates that the ensemble average is over the distribution given by Eq. (4.4). Equation (4.5) gives a simple prescription for evaluating the dynamical correction factors. From a configuration-space Metropolis walk restricted to remain on (or very near) the TST dividing surface for state i, we select a number of configurations. For each of these configurations we assign a velocity to the perpendicular coordinate S, chosen randomly from a Maxwellian-flux distribution $[P(v) \propto |v_i|\exp(-\beta m_s v_i^2/2)]$, and assign a velocity chosen from a Maxwellian distribution $[P(v) \propto \exp(-\beta m v^2/2)]$ to each other coordinate. Each of these N configurations becomes a starting point for a classical trajectory, and we assign a phase to each one according to

$$\text{phase } (I) = \frac{v_i(0)}{|v_i(0)|},$$

so that the phase of a trajectory is positive if it is initially exiting state i, and negative if it is initially entering state i. (Note that these N initial conditions could instead be generated using Bennett's method[6] of selecting snapshots

TABLE I. Monte Carlo TST rate constants (total rate for escape in any direction) and diffusion constants for Rh on Rh(100). The rates have been extrapolated to zero slab width and the error estimates are two standard deviations.

T (K)	$k_{i\to}^{TST}$ (s^{-1})	D^{TST} ($cm^2\ s^{-1}$)
200	3.32×10^{-8}	$(6.38 \pm 0.48) \times 10^{-29}$
300	1.39×10^{-4}	$(2.68 \pm 0.22) \times 10^{-20}$
500	1.30×10^{2}	$(2.49 \pm 0.19) \times 10^{-13}$
1000	2.10×10^{8}	$(4.03 \pm 0.37) \times 10^{-8}$

from the path of a trajectory that is artificially reflected back and forth across the TST dividing surface.) The N trajectories are propagated until $t = \tau_{corr}$, at which time surface-crossing events should have ceased, leaving each trajectory thermalized in some final state. For every state j ($\neq i$) in the system, the elementary rate constant $k_{i\to j}^{el}$ can be computed from

$$k_{i\to j}^{el} = k_{i\to}^{TST}\left[2\sum_{I=1}^{N}\text{phase}\,(I)\theta_j(I)\right], \tag{4.6}$$

where $\theta_j(I) = 1$ if trajectory I resides in state j at time τ_{corr}, and is zero otherwise.

Two properties of Eq. (4.6) are evident. First, $k_{i\to j}^{el}$ can only be nonzero for those states j in which trajectories terminate—as we would expect. Second, it appears possible to obtain a negative value for $k_{i\to j}^{el}$, which would be meaningless. It is easy to prove, however, that for a perfect sampling of trajectories (i.e., if N is made large enough), only nonnegative rates will be computed. This is because in the true canonical ensemble, for every trajectory with negative phase, there is an associated trajectory with positive phase that will terminate in the same state. This can be verified by inspection of Fig. 4; e..g, trajectory 2 is initially entering state l (and thus contributes negatively to $k_{l\to j}^{el}$), but to terminate in state j, it has to exit state l, thus generating the starting point for trajectory 3, which has positive phase and cancels trajectory 2.

V. RHODIUM SURFACE DIFFUSION

Surface diffusion, the migration of an atom or molecule (or collection of molecules) on a solid surface, is an important part of a variety of physical processes, including crystal growth, defect formation, epitaxial layer growth, and heterogeneous catalysis. Understanding the factors that influence the rate and mechanism of this migration is thus of central importance, and has received considerable attention in recent years.[29]

Use of the field ion microscope[30] (FIM), which is capable of observing a single adatom on a clean crystal face, has yielded high-quality surface diffusion constants for a variety of metal-on-metal systems.[31–38] These diffusion constants generally exhibit Arrhenius behavior, with activation energies and preexponentials that vary widely with the choice of metal and crystal face. These results thus allow a test of our qualitative understanding of the microscopic features of the adatom dynamics, and provide quantitative results against which we can test our theoretical methods.

A number of theoretical studies of single-adatom diffusion have appeared, applying either direct MD,[39–45] or some form of TST[24,32,37,46–49] to the problem. All the calculations employed a finite cluster of atoms, bound together by Lennard-Jones or Morse pairwise potentials, to simulate the solid surface. These simulations have proved quite helpful in understanding qualitative features of the diffusion dynamics. For example, Halichioglu *et al.*[45,46] were able to demonstrate that the cross-channel diffusion of Ir on Pt(110) proceeds by a channel-wall knockout mechanism. However, in making quantitative comparisons to experimental diffusion constants, none of these studies has been able to reduce the possible types of error to a single source.

Assuming classical mechanics is valid for describing the dynamics of a particle as heavy as a transition metal atom, the accuracy of a MD simulation should only be limited by the quality of the potential energy function employed. However, at the temperature used in FIM studies (i.e., 350 K and below), the diffusive hops between surface binding sites represent a rare-event process. Thus, MD simulations have only been feasible at much higher temperatures, so that no direct comparisons could be made between theory and experiment. TST diffusion constants have been calculated in the FIM temperature range, but there was no way to tell whether the approximate dynamics or the approximate potential energy function was responsible for the observed disagreement.

The multistate dynamical corrections method derived in Secs. III and IV allows us to directly address this problem, by computing dynamically exact surface diffusion constants at the same temperature as the FIM experiments. Any discrepancy between theory and experiment can then be attributed to the approximate potential function.

The calculations presented here all employ the Lennard-Jones 6-12 template model described previously.[24,42,43] Briefly, this model consists of one or more layers of movable atoms affixed to a rigid template of atoms that has the geometry appropriate for the desired crystal face. The potential energy at each geometry is computed from a Lennard-Jones 6-12 pairwise potential with spherical cutoff

$$V = \sum_{i>j} v'_{ij}, \tag{5.1}$$

where

$$v'_{ij} = \begin{cases} v_{ij}(r_{ij}) - v_{ij}(r_c) & (0 < r_{ij} \leqq r_c) \\ 0 & (r_{ij} > r_c) \end{cases} \tag{5.2}$$

and

$$v_{ij}(r_{ij}) = 4\epsilon_{ij}\left[\left(\frac{\sigma_{ij}}{r_{ij}}\right)^{12} - \left(\frac{\sigma_{ij}}{r_{ij}}\right)^{6}\right]. \tag{5.3}$$

Here r_{ij} is the distance between atoms i and j, ϵ_{ij} and σ_{ij} are the Lennard-Jones well depth and distance parameters for that pair of atoms, and r_c is a cutoff distance. This form for V eliminates the need to calculate interactions between atoms separated by more than r_c, while maintaining a potential that is continuous (though the derivatives are discontinuous at $r_{ij} = r_c$). For the Rh on Rh(100) case considered here, all the interactions are identical ($\sigma_{ij} = \sigma$, $\epsilon_{ij} = \epsilon$), and the parameters were chosen to match previous MD[40–43] and TST[24,49] studies ($\epsilon/k_B = 7830$ K, $\sigma = 2.47$ Å, $r_c = 2.2\sigma$). These values for ϵ and σ were obtained from bulk thermodynamic data.[42] There are 32 atoms per layer in the cluster, with one layer allowed to move and three layers frozen; the total cluster including the adatom thus consists of 129 atoms.

The lattice spacing at all temperatures was chosen to give a nearest-neighbor distance of $2^{1/6}\sigma$ (the minimum in v_{ij}), and periodic boundary conditions were employed.

The TST dividing surface for one binding site is shown in Fig. 6. It is defined by connecting the four atoms around a binding site with planes that extend infinitely in the $+z$ and $-z$ directions. Rather than allowing these planes to move with these four atoms (as in our previous TST studies[24,49]), we simply fixed them to the equilibrium positions of the atoms. This gives a TST surface that depends on the adatom coordinates only, eliminating the need for an effective-mass correction and simplifying the calculation of the trajectory initial velocities. To compute the TST rate constant (Table I), each plane was replaced by a slab with finite thickness b. A Monte Carlo procedure was used to determine the ensemble average in Eq. (4.2), using uniform weighting over the thickness of the slab as a prelimit form for the Dirac delta function. By making independent runs with different values for b, the TST rate was extrapolated to that for a zero-width slab, as shown in Fig. 7. We found that using $b \leqq 0.1$ bohr was sufficient to produce agreement with the $b = 0$ limit. At these low temperatures, accurate evaluation of the Monte Carlo averages requires the use of importance sampling techniques, due to the rare-event nature of the process. We recently presented one such method,[49] but in the present work we had better success with an alternative approach when the slab width was made very small. This new approach exploits the fact that the desired ensemble average can be written as a ratio of partition functions for two states (A and B),

$$\langle \delta_i(0) \rangle_i = \lim_{b \to 0} \left(\frac{1}{b} \frac{Q_B}{Q_A} \right), \tag{5.4}$$

where state A is the whole binding site bounded by the TST dividing surface (the center of the slab), and state B is the hypothetical state generated by restricting the adatom to be inside the slab. The problem thus becomes one of evaluating the free-energy difference between states A and B, and the method is a variation on an existing

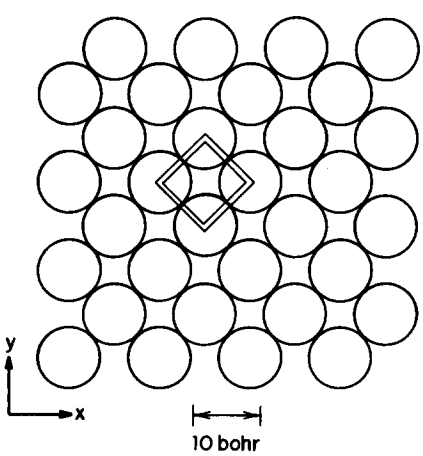

FIG. 6. The LJ template model used for modeling the Rh(100) surface. Only the top layer is shown. For one binding site the TST boundary surface is shown, represented by four finite-width slabs (see the text), which extend infinitely in the $+z$ and $-z$ directions.

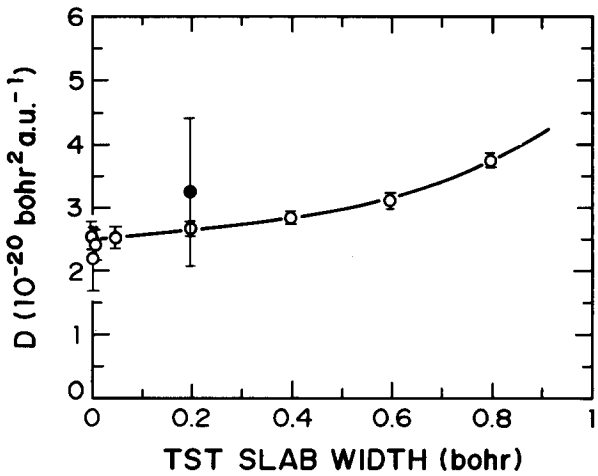

FIG. 7. Extrapolation of the TST diffusion constant at 300 K to zero slab width (see Fig. 6). The error bars are two standard deviations. The shaded point was obtained using TST slabs that moved along with the top-layer atoms (see Ref. 49) and is seen to be in good agreement with the fixed-slab results. The TST rates are shown in Table I.

technique[6] for this type of problem. This method is described in detail elsewhere.[50]

The TST diffusion constant is obtained from

$$D^{\mathrm{TST}} = \frac{l^2}{2d} k_{i\rightarrow}^{\mathrm{TST}}, \tag{5.5}$$

where d is the dimensionality of the space ($d = 2$ in this case; $d = 1$ for channeled surfaces) and l is the distance between adjacent binding sites; i.e., the hop length. In addition to the TST assumption that adatoms crossing the dividing surface do not recross, Eq. (5.5) assumes that successive hops are directionally uncorrelated, so that an adatom has equal probability of exiting to each of the (in this case, four) adjacent sites, regardless of the direction from which it entered. Of course, both of these assumptions are approximations, which can be eliminated using dynamical corrections.

Using the procedure described in Sec. IV, classical trajectories were started from the fixed TST surface, allowing calculation of $k_{i\rightarrow j}^{\mathrm{el}}$ from Eq. (4.6) for all possible binding sites (j) to which the adatom can "hop." The integration was performed using a fourth order Runge–Kutta–Gill algorithm, with a time step of 100 atomic units (1 a.u. = 2.418×10^{-17} s) and an energy rescaling every 11 steps. The highest temperature we report here is 1000 K; above this temperature the time scales (τ_{corr} and τ_{rxn}) begin to be inseparable, so that the elementary rate constants cannot be cleanly extracted. Because of the symmetry of the lattice and the TST surface, it is sufficient to start all trajectories in the same direction from only one of the four TST planes shown in Fig. 6; the fate of the set of trajectories in the true canonical ensemble (which enter and exit state i from all four planes) can be determined from the unique set of trajectories using symmetry considerations.

Figure 8 shows the behavior of 200 trajectories run at 1000 K. At short times, all the trajectories reside in the state that they were entering at $t = 0$ (state B). After ~20 000 a.u., dynamical recrossing events begin to occur. While the majority of trajectories are trapped in state B,

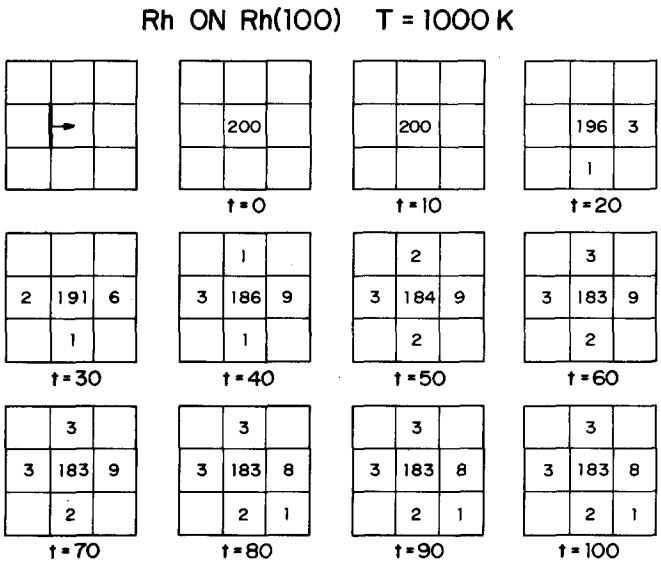

FIG. 8. Time dependence of the state populations resulting from 200 trajectories initiated at the TST plane. All trajectories were initiated from the same TST plane, in the same direction, as indicated by the arrow in the first subfigure. The time units are 10^3 a.u. = 2.42×10^{-14} s. The coordinate system for this representation of the *fcc*(100) lattice is rotated by 45° compared to Fig. 6.

17 of the trajectories exit in various directions before thermalizing in nearby states. These correlated dynamical events have terminated by 80 000 a.u. (continuing 100 of these trajectories until 200 000 a.u. caused only one additional crossing), so that τ_{corr} = 80 000 a.u. Taking $\tau_{rxn} \approx (k^{TST})^{-1}$ leads to

$$\frac{\tau_{rxn}}{\tau_{corr}} = \frac{2.1 \times 10^8}{80\,000} = 2.6 \times 10^3,$$

indicating that the condition of Eq. (3.19) is satisfied. Applying symmetry to generate all possible starting conditions (trajectories entering and exiting from all four sides) and applying Eq. (4.6) leads to the dynamical correction factors shown in Fig. 9. The time dependence is as discussed in Sec. IV, with the correction factors for nonadjacent states initially zero and then rising to a plateau value. The sum of all the f_d values is 0.90,

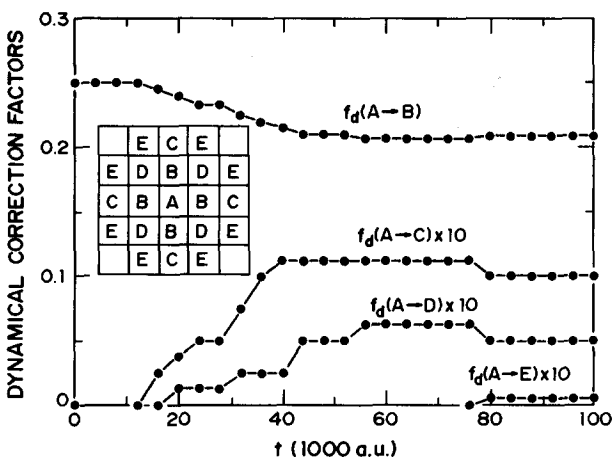

FIG. 9. Dynamical correction factors [Eq. (3.20)] resulting from the 200 trajectories shown in Fig. 8. Symmetry operations were used to construct the additional trajectories present in the total "ensemble," in which trajectories enter and exit from all four directions. (The distribution was also made isotropic by symmetry averaging.)

indicating that the rate at which adatoms escape from a binding site is 10% slower than that predicted by TST.

To compute the dynamically corrected diffusion constant, we replace Eq. (5.5) with a sum over all possible binding sites to which the adatom can directly "hop,"

$$D = \frac{1}{2d} \sum_{j \neq i} k_{i \to j}^{el} l_{ij}^2, \tag{5.6}$$

where l_{ij} is the distance between states i and j. Note that in the limit where the TST assumptions are valid, Eq. (5.6) reduces to Eq. (5.5). Taking the ratio of Eq. (5.6) to Eq. (5.5) leads to the dynamical correction factor for the diffusion constant,

$$\frac{D}{D^{TST}} = \sum_{j \neq i} f_d(i \to j) \left(\frac{l_{ij}}{l}\right)^2. \tag{5.7}$$

These are shown for various temperatures, along with the $f_d(i \to j)$ values, in Table II. While the average hop rate is decreased by the dynamical corrections, the diffusion constant is *increased,* because the average squared length of a hop is increased. Of course, dynamical corrections in general will not necessarily increase D. For example, if the TST surface were poorly chosen, so that $k_{i \to}^{TST}$, and hence D^{TST}, were artificially high, then the dynamical corrections would act to lower D to the classically correct value. Another example is an effect we have observed in Rh on Rh(111) diffusion; at certain temperatures there is an enhanced probability that the adatom that is entering a binding site will bounce off the far wall of this binding site and re-exit in the direction from which it came. On the Rh(100) surface no such effect was observed.

Inspection of Table II also shows that the dynamical effects decrease as the temperature is lowered. This is because at low temperatures the particle typically has just enough energy to pass over the barrier and is easily trapped in the adjacent state, while at higher temperatures there is an increased probability that the particle will have energy in excess of that required to cross the barrier, and may thus make another crossing before this energy is dissipated. This temperature dependence has been observed previously at higher temperatures.[39,44]

An Arrhenius plot of the diffusion constants is shown in Fig. 10, along with the experimental FIM results of Ayrault and Ehrlich.[35] Fitting to the Arrhenius form

$$D = D_0 e^{-E_A/k_B T} \tag{5.8}$$

leads to E_A = 23.82 ± 0.05 kcal/mol and D_0 = (6.6 ± 0.6) × 10^{-3} cm^2 s^{-1}, compared to the FIM values of E_A = 20.2 ± 1.7 kcal/mol and D_0 = 1 × 10^{-3} cm^2 s^{-1}. The theoretical value for D at 300 K is smaller than the experimental values by a factor of 60. As discussed above, this discrepancy can, for the first time, be attributed to the approximate potential function. This LJ potential, which was fit to Rh bulk thermodynamic data, is not necessarily suited to describing atoms on the surface. For two reasons, we make no attempt here to modify the potential to achieve better agreement with experiment. First, the purpose of the present study is to demonstrate the feasibility of obtaining exact dynamical results in the rare-event regime, not to match experiment. Second, any

TABLE II. Dynamical correction factors for Rh on Rh(100). The state designations (i and j) used in $f_d(i \rightarrow j)$ are defined in Fig. 9. N_{traj} is the number of trajectories used to determine the dynamical corrections; N_{corr} is the number of these that come to rest in a state other than B. Note that $f_d(A \rightarrow B) = 0.25$ corresponds to TST.

T (K)	N_{traj}	N_{corr}	$f_d(A \rightarrow B)$	$f_d(A \rightarrow C)$	$f_d(A \rightarrow D)$	$f_d(A \rightarrow E)$	D/D^{TST}
200	100	0	0.25	0.0	0.0	0.0	1.00
300	100	0	0.25	0.0	0.0	0.0	1.00
500	150	1	0.2467	0.0017	0.0	0.0	1.013
1000	200	17	0.2088	0.0100	0.0050	0.000 62	1.060

of a number of arbitrary modifications could be made to the potential to increase the agreement with experiment, but we feel this would have limited meaning. It is possible, however, that calculations like those presented here could be used in conjunction with a variety of other data to generate more accurate potential functions.

Probably the most important result of this Rh on Rh(100) study is that the dynamical corrections are essentially negligible in the temperature range of the FIM experiments (~300 to 330 K). (Even at 1000 K, D/D^{TST} is only 1.06.) While it would be premature to assume this is true of all surface dynamics, it is consistent with other results we have obtained for single metal atoms on metal surfaces. Thus, it appears that future studies of this type can benefit from the significant computational savings of using TST, assuming that a good TST dividing surface can be constructed. For those systems in which there is doubt about the accuracy of TST, the method presented here may be used to obtain the exact dynamics many orders of magnitude more quickly than using full MD simulations.

VI. CONCLUSIONS

We have extended the two-state dynamical corrections formalism to treat the general many-state case. For processes characterized by rare-event dynamics, the method allows the computation of (classical) dynamically exact rate constants between any two states of a system, a task which is unfeasible using direct molecular dynamics. The key to the method is embodied in Eq. (3.12), which expresses the arbitrary elementary rate constant ($k^{el}_{i\rightarrow j}$) as an equilibrium time-correlation function. Equation (3.18) shows that $k^{el}_{i\rightarrow j}$ is simply the TST rate of escape from state i multiplied by a dynamical correction factor, and Eq. (4.6) indicates how this correction factor can be evaluated using molecular dynamics techniques. Dynamical properties of the system may be obtained by following the evolution of a pseudodynamical simulation, in which the system executes a biased random walk from state to state, with weighting governed by the precalculated elementary rate constants. By combining this approach at low temperatures with direct molecular dynamics at high temperatures, dynamical properties may be computed at any temperature. (The middle range of temperatures, where reactive transitions are slightly too frequent to be classified as rare events, then becomes the most computationally intensive.)

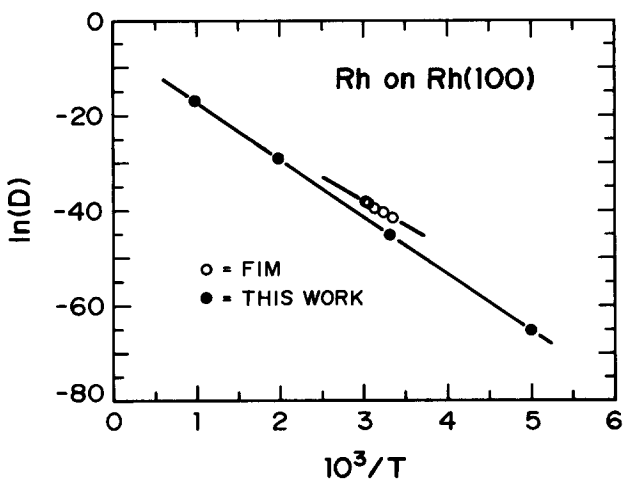

FIG. 10. Surface self-diffusion constants for Rh on Rh(100), plotted in Arrhenius form. The units are D (cm²/s) and T (K). The error bars (two standard deviations) are not shown since they are smaller than the plotted points. The experimental results are from Ref. 35.

An interesting result that emerges from this work is the definition of a rate constant between states which are not adjacent in configuration space. The concept of a "direct" transition between nonadjacent states is intuitively meaningful, and in the rare-event regime, Eq. (3.12) gives a precise definition for this rate.

For the Rh on Rh(100) system, we have calculated the first dynamically exact single-atom diffusion constants in the temperature range of the FIM experiments. The discrepancy between theory and experiment (which is surprisingly small, considering the simplicity of the LJ potential) can now be attributed to the approximate potential function. At 1000 K and below, the dynamical corrections were found to be negligible, indicating that TST is a very good approximation for this type of system. Moreover, we have shown recently[49] that simple harmonic TST, which requires energies at only a few geometries, is a good approximation to exact TST at these low temperatures.[51] Thus, it should be feasible to calculate accurate diffusion constants using *ab initio* electronic structure methods, once relative energies can be obtained with better than 1 kcal accuracy.

Finally, we note that although the Rh diffusion example presented here exhibited only minor dynamical corrections, the method will work equally well if the corrections are large. The method can be applied to any multistate system, as long as molecular dynamics can be run on the potential energy function which is employed. Examples of systems which would benefit from this treatment include the diffusion of atom clusters on a metal surface, the diffusion of vacancies or impurities

through a solid, and the dynamical evolution of a polymer chain.

ACKNOWLEDGMENTS

We wish to thank David Chandler for helpful discussions regarding this work, and J. Winterkamp of Los Alamos National Laboratory's Group ESS-5 for computational support.

APPENDIX

We wish to show that the inverse of the time-zero fluctuation–fluctuation autocorrelation function is indeed given by Eq. (3.11). We take $N = 1$, so that Eq. (3.13) holds, and note that

$$\langle \theta_i^2(0) \rangle = \langle \theta_i(0) \rangle = \chi_i \tag{A1}$$

and

$$\langle \theta_i(0)\theta_j(0) \rangle = \delta_{ij}\chi_i. \tag{A2}$$

For an arbitrary element of the matrix we have

$$\begin{aligned}
&\langle \delta N_i(0)\delta N_j(0) \rangle \\
&\quad = \langle [\theta_i(0) - \chi_i][\theta_j(0) - \chi_j] \rangle \\
&\quad = \langle \theta_i(0)\theta_j(0) \rangle - \chi_i \langle \theta_j(0) \rangle - \chi_j \langle \theta_i(0) \rangle + \chi_i\chi_j \\
&\quad = \delta_{ij}\chi_i - \chi_i\chi_j,
\end{aligned} \tag{A3}$$

as asserted by Eq. (3.10). If the right-hand side of Eq. (3.11) is the inverse of the matrix defined by Eq. (A3), it will satisfy the condition for the inverse of a matrix A:

$$\sum_k (\mathsf{A}^{-1})_{ik}(\mathsf{A})_{kj} = \delta_{ij}. \tag{A4}$$

Inserting Eqs. (A3) and (3.11) into the left-hand side of Eq. (A4) yields

$$\begin{aligned}
&\sum_k^{n-1} (\delta_{ik}\chi_i - \chi_i\chi_k)\left(\frac{1}{\chi_n} + \delta_{kj}\frac{1}{\chi_k}\right) \\
&\quad = \frac{\chi_i}{\chi_n} + \delta_{ij}\frac{\chi_i}{\chi_j} - \sum_k^{n-1} \frac{\chi_i\chi_k}{\chi_n} - \frac{\chi_i\chi_j}{\chi_j} \\
&\quad = \delta_{ij} + \frac{\chi_i}{\chi_n}\left(1 - \sum_k^{n-1} \chi_k\right) - \chi_i \\
&\quad = \delta_{ij},
\end{aligned} \tag{A5}$$

proving Eq. (3.11). The last step in Eq. (A5) made use of

$$\sum_k^n \chi_k = 1.$$

[1] For a recent review, see J. Kushick and B. J. Berne, in *Modern Theoretical Chemistry,* edited by B. J. Berne (Plenum, New York, 1977), Vol. 6.
[2] J. C. Keck, Discuss. Faraday Soc. **33,** 173 (1962); Adv. Chem. Phys. **13,** 85 (1967).
[3] B. Woznick, AVCO-Everett Research Laboratory Report No. RR223, Everrett, Massachusetts, 1965.
[4] R. L. Jaffe and J. B. Anderson, J. Chem. Phys. **54,** 2224 (1971); R. L. Jaffe, J. M. Henry, and J. B. Anderson, *ibid.* **59,** 1128 (1973); J. Am. Chem. Soc. **98,** 1140 (1976), and references therein.
[5] J. B. Anderson, J. Chem. Phys. **58,** 4684 (1973).
[6] C. H. Bennett, in *Diffusion in Solids: Recent Developments,* edited by J. J. Burton and A. S. Nowick (Academic, New York, 1975), p. 73.
[7] C. H. Bennett, in *Algorithms for Chemical Computation,* edited by R. E. Christofferson (American Chemical Society, Washington, D.C., 1977).
[8] D. Chandler, J. Chem. Phys. **68,** 2959 (1978); J. A. Montgomery, Jr., D. Chandler, and B. J. Berne, *ibid.* **70,** 4056 (1979).
[9] J. L. Skinner and P. G. Wolynes, J. Chem. Phys. **69,** 2143 (1978); **72,** 4913 (1980).
[10] See, for example, D. G. Truhlar and B. C. Garrett, Acc. Chem. Res. **13,** 440 (1980), and references therein.
[11] J. E. Adams and J. D. Doll, J. Chem. Phys. **74,** 1467 (1981).
[12] For a recent review, see P. Pechukas, Annu. Rev. Phys. Chem. **32,** 159 (1981).
[13] A. Marcelin, Ann. Phys. (Paris) **3,** 120, 185 (1915).
[14] R. L. Jaffe, Chem. Phys. **40,** 185 (1979).
[15] R. N. Porter, D. L. Thompson, L. M. Raff, and J. M. White, J. Chem. Phys. **62,** 2429 (1975).
[16] J. A. Montgomery, Jr., S. L. Holmgren, and D. Chandler, J. Chem. Phys. **73,** 3688 (1980).
[17] E. K. Grimmelmann, J. C. Tully, and E. Helfand, J. Chem. Phys. **74,** 5300 (1981); J. C. Tully, Surf. Sci. **111,** 461 (1981).
[18] J. E. Adams and J. D. Doll, Surf. Sci. **103,** 472 (1981); J. Chem. Phys. **80,** 1681 (1984).
[19] J. E. Adams and J. D. Doll, Surf. Sci. **111,** 492 (1981).
[20] This estimate assumes the use of the fastest currently available computer.
[21] B. J. Berne and G. D. Harp, Adv. Chem. Phys. **17,** 63 (1970).
[22] J. D. Doll, J. Chem. Phys. **74,** 1074 (1981).
[23] Of course, Eq. (2.16) does depend on state B in the sense that it depends on the location of the boundary line ($x = q$) between state A and state B.
[24] A. F. Voter and J. D. Doll, J. Chem. Phys. **80,** 5832 (1984).
[25] Harold S. Johnston, *Gas Phase Reaction Rate Theory* (Ronald, New York, 1966), p. 48.
[26] N. Metropolis, A. Rosenbluth, M. N. Rosenbluth, A. Teller, and E. Teller, J. Chem. Phys. **21,** 1087 (1953).
[27] J. P. Valleau and S. G. Whittington, in *Modern Theoretical Chemistry,* edited by B. J. Berne (Plenum, New York, 1977), Vol. 5.
[28] For applications of Monte Carlo to calculating TST rates, see Refs. 11, 24, and 29.
[29] For a recent review, see G. Ehrlich and K. Stolt, Annu. Rev. Phys. Chem. **31,** 603 (1980).
[30] E. W. Muller and T. T. Tsong, *Field Ion Microscopy, Principles and Applications* (Elsevier, New York, 1969).
[31] G. Ehrlich and F. G. Hudda, J. Chem. Phys. **44,** 1039 (1966).
[32] G. Ehrlich and C. F. Kirk, J. Chem. Phys. **48,** 1465 (1968).
[33] D. W. Bassett and M. J. Parsley, J. Phys. D **3,** 707 (1970).
[34] W. R. Graham and G. Ehrlich, Phys. Rev. Lett. **31,** 1407 (1973); Thin Solid Films **25,** 85 (1975).
[35] G. Ayrault and G. Ehrlich, J. Chem. Phys. **60,** 281 (1974).
[36] P. Cowan and T. T. Tsong, Phys. Lett. A **53,** 383 (1975); 22nd International Field Emission Symposium, Atlanta, Georgia, 1975.
[37] D. W. Basset and P. R. Webber, Surf. Sci. **70,** 520 (1978).
[38] P. G. Flahive and W. R. Graham, Surf. Sci. **91,** 463 (1980).
[39] M. R. Mruzik and G. M. Pound, J. Phys. F **11,** 1403 (1981).
[40] H. K. McDowell and J. D. Doll, Surf. Sci. **121,** L537 (1982).
[41] J. D. Doll and H. K. McDowell, Surf. Sci. **123,** 99 (1982).
[42] J. D. Doll and H. K. McDowell, J. Chem. Phys. **77,** 479 (1982).
[43] H. K. McDowell and J. D. Doll, J. Chem. Phys. **78,** 3219 (1983).
[44] J. C. Tully, G. H. Gilmer, and M. Shugard, J. Chem. Phys. **71,** 1630 (1979).
[45] S. H. Garofalini and T. Halichioglu, Surf. Sci. **104,** 199 (1981); **112,** L775 (1981); also see H. P. Bonzel, *ibid.* **121,** L531; S. H. Garofalini and T. Halichioglu, *ibid.* **121,** L535 (1982).
[46] T. Halichioglu and G. M. Pound, Thin Solid Films **57,** 241 (1979).
[47] P. Wynblatt and N. A. Gjostein, Surf. Sci. **22,** 125 (1970).
[48] J. R. Banavar, M. H. Cohen, and R. Gomer, Surf. Sci. **107,** 113 (1981).
[49] A. F. Voter and J. D. Doll, J. Chem. Phys. **80,** 5814 (1984).
[50] A. F. Voter and J. D. Doll, J. Chem. Phys. (in press).
[51] The agreement between simple TST and exact TST should be even better than that shown in Ref. 49 if all force constants are evaluated at the minimum and the saddle point. This can be accomplished with current *ab initio* techniques.